DOI: 10.1002/cbic.200800247

Peptide-Grafted Nanodiamonds: Preparation, Cytotoxicity and Uptake in Cells

Stéphanie Vial,[a] Christelle Mansuy,[a] Sandrine Sagan,[a] Theano Irinopoulou,[b] Fabienne Burlina,[a] Jean-Paul Boudou,[c] Gérard Chassaing,[a] and Solange Lavielle*[a]

Nanodiamonds that were prepared by high pressure/high temperature were functionalised with biomolecules for biological applications. Nanodiamonds (NDs, $\leq$35 nm) that were coated by silanisation or with polyelectrolyte layers were grafted with a fluorescent thiolated peptide via a maleimido function; this led to an aqueous colloidal suspension that was stable for months. These substituted NDs were not cytotoxic for CHO cells. Their capacity to enter mammalian cells, and their localisation inside were ascertained after labelling the nucleus and actin, by examining the cells by confocal, reflected light and fluorescence microscopy.

Introduction

The design of nanoparticles that are suitably functionalised for applications in biology or medicine is an ongoing challenge for both chemists and biologists. Nanoparticles, such as quantum dots,[1,2] gold nanoparticles[3–5] or carbon-based materials[6–9] offer, in addition to their remarkable physical properties, the possibility to be functionalised by biomolecules; this makes them suitable for sensing, detection, diagnostic, and/or therapeutic applications. Recently, quantum dots,[10] which have unique size-dependent fluorescence properties, have been designed for biological imaging. However, their possible toxicity still remains a major concern for in vitro and in vivo applications.[10] Nanodiamonds (NDs) are also candidates for biomedical applications because of their intrinsic or induced fluorescence[11–13] and biocompatibility.[14] They can be prepared either by detonation, or by high-temperature–high-pressure (HPHT) procedures. Both processes lead to the formation of impure layers on their surfaces, which need to be cleaned by harsh acidic treatment; this generates carboxylic groups on the nanodiamond (cND) surface. These cNDs can exhibit two types of fluorescence (fNDs): a natural green fluorescence[12] and an induced bright-red fluorescence.[11,13,15] The latter is observed on type Ib diamonds (HPHT) with a size as small as 25 nm,[15] and is associated with nitrogen-vacancy centre defects that are produced by high-energy ion beam irradiation and subsequent thermal annealing. The cytotoxicity and cellular uptake of cNDs and fNDs have been studied previously,[11–14] and it has been shown that they are biocompatible with a variety of cells and localise in the cytoplasm. Such cNDs, especially detonation NDs, have been functionalised with biomolecules through either adsorption by electrostatic and/or hydrophobic interactions[16–19] or covalent linkage.[16,20–22] In a few reports, the activities and/or the intracellular locations of these conjugated NDs were analysed.[17,18,22]

One of the most critical points that has limited the use of NDs in biological applications is the preparation of a functionalised cND colloidal suspension that is stable over long periods of time. In addition, the location of NDs inside cells remains to be defined unambiguously (distinction between internalised and stuck on the membrane). The preparation of intrinsic fluorescent NDs is also a limiting step. Their production by either high-energy electron or proton irradiation is, up to now, feasible only on a small scale, and leads to fNDs with an average size between 20 and 100 nm. Because only a few groups[11–13] have briefly described their preparation and their use, most of the work suffers from the rarity of intrinsic fNDs, and from a lack of information regarding the suspension stability during the functionalisation steps.

We assumed that once the chemistry was mastered on well-defined ND species (commercially available, nonfluorescent ND with an average size of 20–40 nm) it would be easy to transfer this knowledge to intrinsic fNDs as soon as a "large-scale" production was feasible. Therefore, the work herein describes: 1) the functionalisation and the characterisation of $\leq$35 nm nonfluorescent cNDs and 2) their use in toxicity and transport studies in living cells after the grafting of a fluorescent model peptide. We chose to introduce a nonpenetrating fluorescent peptide for the tracking of the nanoparticles on or inside cells.

[a] *Dr. S. Vial,[+] Dr. C. Mansuy,[+] Dr. S. Sagan, Dr. F. Burlina, Dr. G. Chassaing, Prof. Dr. S. Lavielle*
UPMC Université Paris 06, CNRS-UMR 7613
Synthèse, Structure et Fonction de Molécules Bioactives
case courrier 182, 4 Place Jussieu, 75005 Paris (France)
Fax: (+33) 1-44-27-55-35
E-mail: solange.lavielle@upmc.fr

[b] *Dr. T. Irinopoulou*
UPMC Université Paris 06, INSERM, UMR-S 839
Institut du Fer à Moulin
17, Rue du Fer à Moulin 75005 Paris (France)

[c] *Dr. J.-P. Boudou*
UPMC Université Paris 06, CNRS-UMR 7618
Biogéochimie des Milieux Continentaux
4 Place Jussieu, 75005 Paris (France)

[+] *These authors contributed equally to this work.*

Supporting information for this article is available on the WWW under http://www.chembiochem.org or from the author.

The strategies to chemically modify the cND surface are rather limited because cNDs easily aggregate in organic solvents. The strategy that we have adopted to graft a peptide involves three steps: 1) functionalisation of the cND surface with amino groups by coating them with an organosilane or a polyelectrolyte, 2) coupling of a bifunctionalised linker to 3) introduce a thiolated tripeptide via a maleimide group (Scheme 1). At each step the nanoparticles were fully characterised and the major aim was to maintain a colloidal suspension after peptide grafting in order to obtain a suitable ND size for cellular internalisation studies. The chemical and colloidal stabilities of the functionalised NDs were analysed over a long period of time (six to nine months). Cytotoxicity (by measuring dehydrogenase activity) and cell entry (by using confocal microscopy) of the resulting ND–tripeptide conjugates versus the free tripeptide were then studied with CHO cells.

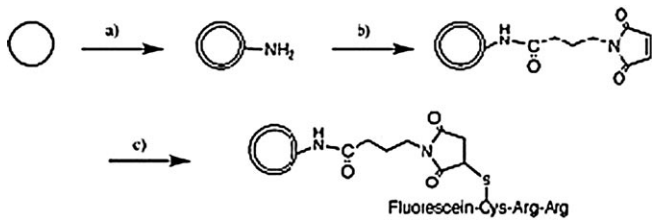

Scheme 1. Functionalisation of cNDs with a fluorescent model tripeptide. a) Silanisation route: octyl-β-D-glucopyranoside (OG) then 3-(aminopropyl)-trimethoxysilane (APS). Polyelectrolyte route: polyallylamine hydrochloride (PAH); b) maleimidobutyric acid (MBA), EDC; c) peptide fluorescein–Cys–Arg–Arg.

Results and Discussion

Preparation of substituted NDs: synthesis and characterisation

The commercially available Van Moppes NDs (SYP 0.05) have a size that is close to 35 nm, as confirmed by transmission electronic microscopy. This diamond powder was first treated in acidic media to purify the ND surface and to concomitantly introduce carboxylic groups onto this ND surface. Because of the resulting highly negative surface charge, a stable aqueous colloidal suspension of cNDs was obtained after mild ultrasonication. The characteristics of these cNDs are reported in Table 1.

The use of organosilanes or polyelectrolytes for surface functionalisation has been described in the literature for different kinds of nanoparticles (e.g., magnetic, luminescent, semiconductor). To obtain a homogeneous functionalisation of cNDs with amino groups, two strategies of coating were studied: 1) silanisation by using 3-(aminopropyl)trimethoxysilane (APS; route 1), and 2) polyelectrolyte adsorption by using polyallylamine (PAH; route 2). The silanisation route[20] has already been described with aggregated detonation nanodiamonds. In our study, the starting HPHT cNDs are individual particles in solution. Silanisation involves the reaction between hydroxyl groups and an organosilane. The hydroxyl groups at the surface of cNDs were introduced by adsorption of octyl-β-D-glucopyranoside (OG) onto cNDs. OG is a nonionic surfactant that ensures better stability of cNDs in acetone compared to "nude" cNDs in organic solvents. The silanisation reaction was performed in acetone to control alkoxides hydrolysis, which occurs during this reaction, to coat homogeneously the cNDs and avoid the formation of single silica particles. This was performed by dropwise addition of APS (under sonication) onto OG-coated cNDs, and allowed functionalisation by amino groups. After washing, a final stable aqueous suspension of amino-substituted silanised-cNDs was obtained. Alternatively, the starting cNDs were treated with the PAH polyelectrolyte ($M_W = 10\,000$).[23] Functionalisation that is based on the adsorption of amino compounds, such as poly-L-lysine, on cND surface has already been reported by Huang and Chang.[16] They studied the possibility of grafting cytochrome c on the available amino functions of adsorbed poly-L-lysine via a linker. In our study, we chose to coat the cND surface with a positively charged polyelectrolyte (PAH) by taking advantage of the electrostatic interaction between the carboxylate functions of the cNDs and the ammonium groups of PAH. The amino substitution was determined by using the Kaiser test;[24] the substitution degree was close to 100 and 200 $\mu mol\,g^{-1}$ for routes 1 and 2, respectively. Both procedures for the introduction of amino groups on the cND surface were highly reproducible and gave stable aqueous suspensions (Table 1).

Both amino substituted cNDs were then treated with the bifunctional maleimidobutyric acid linker (MBA) activated beforehand with 1-(3-dimethylaminopropyl)-3-ethylcarbodiimide hydrochloride (EDC). The maleimide moiety is commonly used in

Table 1. Characterisation of NDs at each functionalisation step.

Functional group on ND surface	Starting cNDs	OG	APS	Maleimide	Fluo–CRR[a]	PAH	Maleimide	Fluo–CRR[b]
diameter [nm][c]	55	100	110	120	130	70	n.d.	150
zeta [mV]	−40	n.d.[d]	−27	−15	−25	40	n.d.[d]	−20
concentration [$g\,L^{-1}$]	1.0	0.6	0.6	0.3	0.2	0.8	0.6	0.2
pH	5.5	n.d.[d]	9.5	5.5	7.0	6	6	6.5
amine [$\mu mol\,g^{-1}$]	0	n.d.[d]	100	6	n.d.[d]	220	30	n.d.[d]
stability	H_2O	acetone	H_2O	H_2O	H_2O	H_2O		H_2O

[a] cND–APS–Fluo–CRR; [b] cND–PAH–Fluo–CRR; [c] hydrodynamic; [d] not determined.

peptide/protein chemistry as a linker to form a thioether bond with thiolated molecules by Michael addition. The successful introduction of a maleimide onto the coated ND surface was supported by the Kaiser assay, which showed an important, if not total, decrease in the amino substitution of the nanoparticles (Table 1). At this stage, however, the colloidal suspensions were less stable regardless of the initial coating strategy (silanisation or polyelectrolyte). This loss of stability was related to the zeta potential: −15 mV for the silanisation route and was not detectable for the polyelectrolyte route. Thus, the tripeptide fluorescein–Cys–Arg–Arg (Fluo–CRR) was immediately coupled to both types of functionalised cNDs to yield cND–APS–FluoCRR and cND–PAH–FluoCRR.

For each step of the preparation, Table 1 displays the diameter of the NDs, which was measured by dynamic light scattering (DLS), the zeta potential, the amount of amino groups that were grafted onto the surface, as well as the stability of the different ND suspensions.

The different functionalisation steps were also characterised by IR spectroscopy. Treatment of the starting NDs in acidic media led to the introduction of functional groups onto their surface, as attested by the IR spectrum.[19,25] A band at 1790 cm^{-1} was assigned to carbonyl stretching modes, and weak bands at 2917 and 2836 cm^{-1} correspond to the asymmetric and symmetric stretching of C–H vibrations, respectively. A broad band between 3000 and 3600 cm^{-1} and another at 1630 cm^{-1} can be attributed to the O–H bending of adsorbed water. The peaks at 1093 and 1400 cm^{-1} can be assigned to the presence of ether-like groups on the surface. The silica layer on the NDs obtained by the silanisation route (cND–APS particles) is evidenced by the Si–O–Si stretching vibrations at 1130 and 1032 cm^{-1}.[26] The band at 1575 cm^{-1} indicates the presence of primary amines, which are provided by APS. In the case of the polyelectrolyte route (cND–PAH particles),[27] the adsorption of PAH is supported by the presence of the 1571 and 1497 cm^{-1} bands, which correspond to the amides I and II, respectively. The IR spectrum after the introduction of the maleimide moiety[28,29] showed an intense peak at 1700 cm^{-1}, which is due to the asymmetric stretching mode, and a weak peak at 1780 cm^{-1} that is related to the symmetric stretching mode of the imidyl group; this signifies the presence of the cross-linker. Furthermore, the band at 1540 cm^{-1} supports the formation of a covalent amide bond between the amino groups on the ND surface and the carboxylic function of MBA. Finally, immobilisation of the tripeptide Fluo–CRR was confirmed by FTIR analysis. The bands at 1642 and 1575 cm^{-1} correspond to the stretching and deformation mode of the C=O (amide I) and N–H (amide II) bonds, respectively. The bands at 1465 and 1350 cm^{-1} are related to C–H vibrations of the CH_2 groups.

The zeta potentials of the starting and functionalised cNDs were also measured for both routes (Table 1). The initial cNDs showed a zeta potential close to −40 mV, which indicates the presence of carboxylate functions on the ND surface. This highly negative zeta potential led to good stability of the ND suspensions in aqueous solvent, but aggregation of the cNDs was observed for pH values below two or above eleven. Zeta potentials higher than +25 or below −25 mV are considered to be the threshold values for stable colloidal suspensions. After silanisation, the zeta potential remained negative (−27 mV) despite the introduction of amino groups onto the surface, whereas with polyelectrolytes the ammonium groups shifted the zeta potential to a highly positive value (+40 mV; Figure 1).

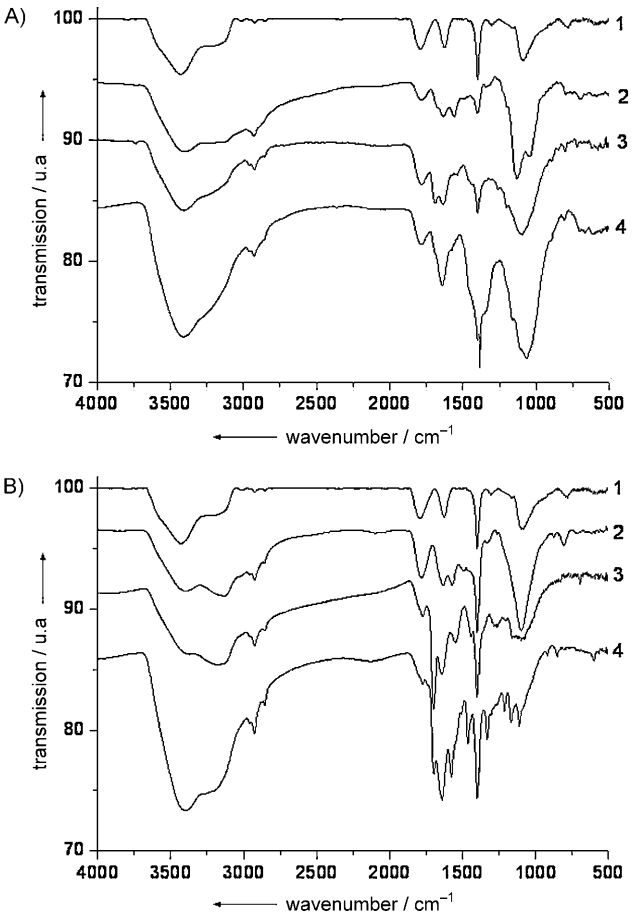

Figure 1. IRFT spectra of functionalised cNDs. A) Silanisation route; 1: cNDs; 2: cNDs–APS; 3: cNDS–APS–MBA; 4: cNDS–APS–MBA–peptide. B) Polyelectrolyte route; 1: cNDs; 2: cNDS–PAH; 3: cNDS–PAH–MBA; 4: cNDS–PAH–MBA–peptide.

After introduction of the maleimide onto the silanised NDs the zeta potential further increased to −15 mV. Finally, grafting the Fluo–CRR peptide imparted a net negative charge close to −25 mV to the silanised NDs, which ensured satisfactory electrostatic repulsions to stabilise the suspension. For the PAH procedure, the zeta potential of the final cND–PAH–FluoCRR was also negative (−20 mV). It is rather difficult to rationalise these zeta variations. The global charge of the Fluo–CRR peptide that is linked via a thioether bond should be close to neutral depending on the local pH on the ND surface with the tripeptide containing two guanidiniums, one carboxylate and the N-terminal carboxyfluorescein. The zeta potentials might not reflect solely the charges on the surface but also the hydratation propensity, and the environmental hydrophobicity might

also be one of the parameters that governs the value and the sign of the zeta potential.

The different steps to functionalise the NDs led to an increase of the hydrodynamic diameter, as determined by DLS measurements, from 55 nm to 130–150 nm once the peptide had been grafted (Table 1). This increase in size might not only be related to the chemicals that are grafted on the ND surface. The size increase could result from a decrease in the stability of the nanoparticle suspensions in the first steps, when OG was added in acetone for the silanisation route or, when maleimide was introduced, for the polyelectrolyte coating. It should be noted that aggregation of NDs increased in organic solvent.

The final aqueous suspensions of peptide-substituted cNDs were stable for several months, as shown by the zeta potentials and the hydrodynamic diameters determined by DLS over this period of time.

Cytotoxicity and cell uptake of the substituted NDs

The cytotoxicity and capability of both peptide-grafted cNDs to enter Chinese hamster ovary (CHO) cells were then studied. Cytotoxicity was evaluated by the decrease in intracellular dehydrogenases activity[30] (CCK-8 cell-counting kit). Cytotoxicity was assayed for different amounts of conjugated cNDs up to a concentration of 40 $\mu g\,mL^{-1}$ (see the Supporting Information). This concentration was the highest to be tested because of the concentration of the ND colloidal solutions. To obtain a 40 $\mu g\,mL^{-1}$ concentration, 20 μL of the ND colloidal suspension in water was added to the cells (in 100 μL of medium). Larger volumes of the ND vehicle (water) alone caused cell death. It has to be noted that the NDs were left in contact with the cells during the whole incubation time (24 to 72 h). Under these conditions, no cytotoxicity was observed after either 24 or 72 h incubation of the cells (1000–5000 cells per well) with any of the prepared (40 $\mu g\,mL^{-1}$) nanoparticles (cND, cND–APS, cND–PAH, peptide-grafted cNDs).

In the cellular uptake experiments, the distinction between extracellular and intracellular particles was difficult to achieve when large amounts of NDs were used. Indeed, NDs accumulated on the cell surface with time, and were difficult to wash out after incubation. Therefore, these NDs aggregated on the cell-surface and disturbed the visualisation of the internalised NDs (Figure 2).

To unambiguously distinguish membrane-bound from internalised NDs, lower concentrations of NDs were tested with short incubation times. Our data unambiguously establish that the peptide-grafted cNDs were indeed inside the cells. A low ND concentration (6 $\mu g\,mL^{-1}$) and a short incubation time (1 h) were used; the actin (TRITC, red) and nucleus (TO-PRO-3 iodide, blue) were labelled so that NDs could be localised inside the cell. To confirm that the green fluorescence could be attributed to the peptide-grafted nanodiamonds, differential interference contrast, reflection and green fluorescent images were taken from a single confocal section in the middle of a cell (Figure 3 and 4). The physical association of the fluorescent peptide with the NDs was evidenced with the overlay of reflection and fluorescence images (Figure 4). Differ-

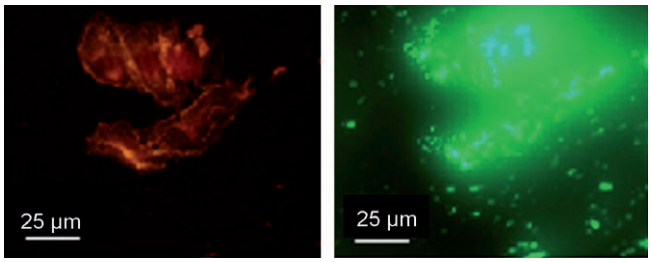

Figure 2. Images showing the cell-surface accumulation and aggregation of cND–PAH–Fluo–CRR (12 $\mu g\,mL^{-1}$; right) after 2 h incubation with CHO cells; actin was labelled (left) to visualise the cells. Images were obtained through a Nikon Eclipse TE2000s microscope with a 60×/0.5–1.25 PLAN FLUOR objective.

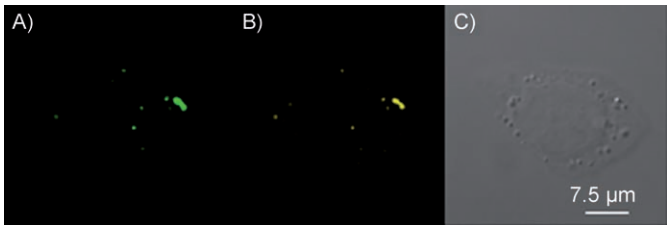

Figure 3. Correlation between fluorescein and cNDs. A) Fluorescence (fluorescein), and B) reflection images from a single confocal section in the middle of a cell, and C) the corresponding differential interference contrast image. The cND–PAH–Fluo–CRR (6 $\mu g\,mL^{-1}$) was incubated with CHO cells for 1 h. The images were collected with a LEICA SP2 confocal laser scanning microscope with a 63× (NA 1.32) objective.

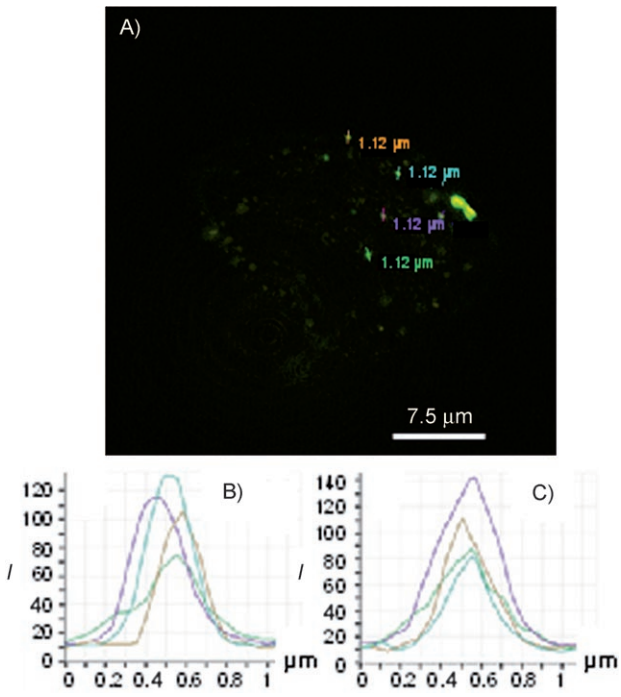

Figure 4. Visualisation of the peptide-grafted cNDs (6 $\mu g\,mL^{-1}$) incubated for 1 h with CHO cells. A) Overlay of fluorescent and reflection images of Figure 3. Different line regions traced on individual (diffraction limited) particles. B) Reflection and C) fluorescent intensity (*I*) graphs for all regions.

ent lines were traced, and the associated reflection and fluorescence intensities were determined. The superposition of peaks corresponding to the two modes of detection confirmed the tight association of the fluorescent peptide with cNDs. Therefore, it was ascertained that the detection of green fluorescence in cells corresponds to the peptide-grafted cNDs.

Cells that were incubated with NDs (6 $\mu g\,mL^{-1}$ for 1 h) were further examined by confocal microscopy. From a series of optical sections (0.8 μm apart in the *z* axis; Figure 5) the appearance and disappearance of green fluorescence, which corresponds to the NDs in the cells, could be clearly observed. In contrast, the free peptide (fluorescein–CRR) was not internalised into cells by itself (not shown). These results indicated that the functionalised nanoparticles were internalised into the cells and that they did not simply accumulate on the surface. Figure 6 shows the whole cell (48 optical sections 0.2 μm apart), which was visualised by using the blending volume rendering technique. Nanoparticles were mostly localised in the cytoplasm and were found to be embedded in the actin cytoskeleton of CHO cells (Figures 5 and 6). According to the size of these NDs, their internalisation likely occurred by endocytosis.

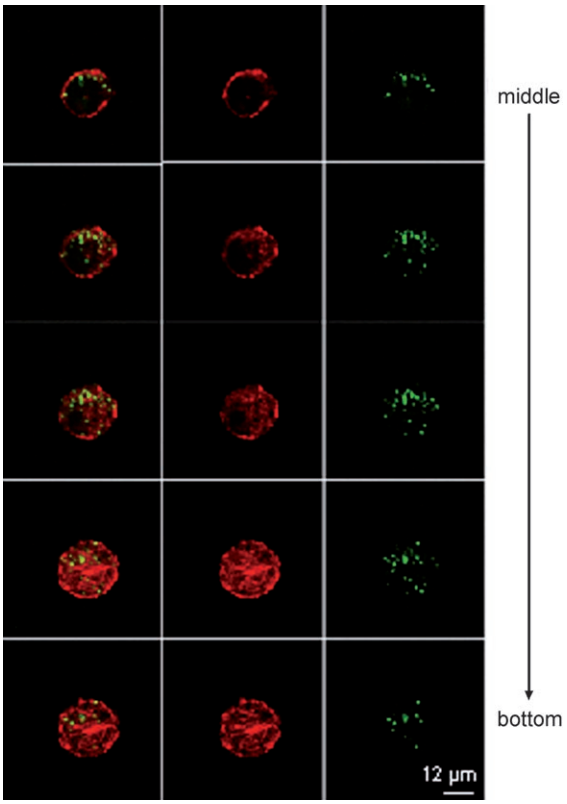

Figure 5. Visualisation of cND–PAH–Fluo–CRR (6 μg incubated for 1 h with CHO cells). Different confocal images from the bottom to the middle of cell (0.8 μm apart) were collected with a LEICA SP2 confocal laser-scanning microscope with a 100× (NA 1.4) objective. Right-hand column: fluorescent peptide-grafted cNDs, middle column: actin; left-hand column: merged images.

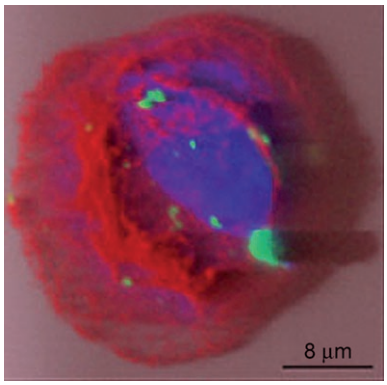

Figure 6. Actin-embedded cND–PAH–Fluo–CRR in the cytoplasm of CHO cells. Forty-eight optical sections (0.2 μm apart) were collected. This image represents the whole cell, which is visualised by blending volume rendering (Imaris 4.0 software, Bitplane, Switzerland). Blending volume rendering shows the colour by blending all values along the viewing direction and including their transparency; light from the left was used.

Conclusions

In conclusion, we have developed two functionalisation routes that allow the grafting of peptides on NDs and preserve the colloidal state for the final peptide-grafted cNDs. These ND suspensions were found to remain stable over at least several months. These modified NDs are nontoxic and enter mammalian cells efficiently. Although the fine localisation of these peptide-grafted cNDs in cells remains to be fully studied, their internalisation was unambiguously established and they were found to be embedded in the actin cytoskeleton. Thus, NDs are promising candidates for the attachment of multiple bioactive compounds and their delivery into cells, and functionalised fluorescent NDs will allow us to study their trafficking inside cells.

Experimental Section

Materials: Octyl-β-D-glucopyranoside (OG, ≥98%), (3-aminopropyl)trimethoxysilane (APS, ≥97%), 4-maleimidobutyric acid (MBA, ≥98%) were purchased from Aldrich; 1-(3-dimethylaminopropyl)-3-ethylcarbodiimide hydrochloride (EDC) was obtained from VWR; 5(6)-carboxyfluorescein (≥95%), preloaded Fmoc–Arg(Pbf)–Novasyn resin, Fmoc–Arg(Pbf)–OH and Fmoc–Cys–(Trt)–OH were purchased from Novabiochem.

Fluorescein–Cys–Arg–Arg–COOH: The tripeptide, CRR–COOH, was assembled by stepwise solid-phase synthesis with an ABI 433A peptide synthesiser (Applied Biosystems) by using the standard Fmoc strategy (Fmoc–Arg(Pbf)–Novasyn resin, 0.21 $mmol\,g^{-1}$) at Plateforme d'Ingénierie des Protéines Synthèse Peptidique (IFR 83), UPMC, Paris. Coupling to the resin was performed by activation of the amino acids (10 equiv) with HBTU, iPr_2EtN and *N*,*N*′-dicyclohexalcarbodiimide in NMP. Piperidine was used to remove the Fmoc groups and Ac_2O was used for capping. Coupling of the fluorescent probe was done manually by using 5,6-carboxyfluorescein (2.5 equiv) that had been activated with a 1 M HOBT solution in NMP (2.5 equiv,) and *N*,*N*′-diisopropylcarbodiimide (DIC; 2.5 equiv)

in DMF. The reaction was allowed to proceed for 16 h at room temperature. A negative Kaiser's test confirmed the total coupling. The final peptidyl–resin was cleaved from the resin by treatment with trifluoroacetic acid (TFA, 94%), ethanedithiol (EDT, 2.5%), triisopropylsilane (TIS, 1%) and H_2O (2.5%) for 2 h. After filtration and evaporation, the peptide was first precipitated in cold diethyl ether, then resolubilised in a mixture of AcOH/H_2O (1:9), for purification by reverse-phase preparative HPLC on a C8 column. The pure fractions were pooled and after lyophilisation the peptide Fluo–CRR was characterised by MALDI-TOF mass spectroscopy.

Functionalisation of cNDs: After acid treatment, an aqueous colloidal suspension (1 g L^{-1}) of cNDs (SYP 0–0.05, $\leq$35 nm, Van Moppes) was obtained by ultrasonication (3 h, 300 W).

cNDs coated by silanisation, cND–APS–Fluo–CRR: The transfer of the cNDs from H_2O (20 mL) to acetone was done after the addition of a few drops of a sat. aq. NaCl solution. After centrifugation, the cNDs were redispersed in acetone (30 mL) and OG surfactant (10 mL, 20 mM in H_2O) was immediately added under sonication (1 h, sonication bath). Excess OG was removed by washing/centrifugation cycles (3×). NDs were redispersed in acetone (30 mL) and sonicated (1 h). Silanisation was performed by the dropwise addition under sonication of APS (212 μL), the solution was sonicated (1 h) then stirred (15 h, room temperature). The NDs were washed with acetone (3×), then H_2O (3×), and redispersed in H_2O (30 mL). After sonication (1 h), a stable suspension of amino-substituted NDs was obtained (0.6 g L^{-1}). 4-Maleimido butyric acid (MBA, 30 mg) was activated with 1-ethyl-3-(3-dimethylaminopropyl)-carbodiimide (EDC, 1 g) for 30 min in 10 mL. The resulting solution was added under sonication to the cNDs (25 mL, 15 mg). The suspension was sonicated (15 min) and stirred (16 h). After washing/centrifugation cycles (H_2O, 3×) with increasing speeds (up to 10000 rpm), the resulting cNDs were redispersed in H_2O (25 mL), and sonicated (1 h) to obtain a suspension, (0.4 g L^{-1}). The tripeptide (800 μL in H_2O, 1 mM) was immediately added to the suspension (25 mL) and the mixture was stirred for 18 h in the dark. After three centrifugation/washing cycles, the NDs were redispersed in H_2O (15 mL) and sonicated (15 min). A last centrifugation step (5 min, 1500 rpm) was performed and the suspension of cND–APS–Fluo–CRR (0.2 g L^{-1}) was stored at 4 °C.

NDs coated with polylectrolytes cND–PAH–Fluo–CRR: The cND solution (20 mL) was added dropwise to a vigorously stirred PAH solution (20 mL, M_W = 10000, 1 g L^{-1}, 3 mM NaCl), which had been previously sonicated for 15 min. The mixture was stirred (18 h, room temperature), then centrifuged/washed (3×) with increasing speeds (up to 10000 rpm) and redispersed in H_2O (15 mL). The activation of MBA (50 mg) with EDC (1 g) was performed as described above. The resulting solution was added under sonication to a suspension of amino-substituted NDs, which had been adjusted previously at pH 7 with NaOH. The suspension was stirred, overnight, centrifuged/washed (3×) and then redispersed in H_2O (15 mL). Because the final suspension was rather unstable the tripeptide was immediately grafted on this ND solution (12 mL) as described above. Finally, the cND–PAH–Fluo–CRR was redispersed in H_2O (20 mL, 0.2 g L^{-1}) and stored at 4 °C.

Kaiser assay:[24] Phenol/EtOH (75 μL; 80 g in 20 mL), pyridine/KCN (1 mM; 98:2, 100 μL) and ninhydrine/EtOH (75 μL; 1 g in 20 mL) were added to dried amino-substituted NDs (0.1–0.5 mg). The suspension was heated at 100 °C for 5 min then cooled with H_2O/EtOH (2 mL, 4:6). The solution was centrifuged at 13000 rpm for 5 min to remove the ND particles. The concentration of amino groups that were present on the ND surface was determined with this solution at 570 nm and calculated with Equation (1):

$$\mu\text{mol g}^{-1} = \frac{(\text{Abs}_{\text{sample}} - \text{Abs}_{\text{blank}}) \times \text{volume (mL)} \times 10^6}{\varepsilon \times \text{sample weight (mg)}} \quad (1)$$

with the extinction coefficient $\varepsilon = 19700\ \text{M}^{-1}\,\text{cm}^{-1}$.

Particle characterisation: The hydrodynamic diameter of the nanoparticles and the surface charge were measured by dynamic light scattering (DLS) and zetametry with the Zetasizer Nano ZS from Malvern (Worcestershire, UK). Fourier transform infrared (FTIR) spectra were acquired by using a Nicolet Magma 860 spectrometer with a resolution of 4 cm^{-1}. For FTIR analysis, dried nanoparticles (2 mL), which were obtained after overnight lyophilisation, were mixed with KBr (100 mg) and the mixture was pressed into a pellet.

Cell culture: Chinese hamster ovary (CHO) K1 cells were cultured in Dulbecco's modified Eagle's medium (DMEM) that was supplemented with foetal calf serum (FCS, 10%), penicillin (100000 IU L^{-1}), streptomycin (100000 IU L^{-1}) and amphotericin B (1 mg L^{-1}), and incubated in a humidified atmosphere with 5% CO_2 at 37 °C.[30]

Cytotoxicity: Dehydrogenase activity detection in viable cells was measured with the colorimetric assay cell counting kit-8 (CCK-8 from Dojindo's).[30] CHO cells (5000 in 100 mL culture medium) were seeded in 96-wells plates, 24 h before cytotoxycity assays. NDs were added to cells and incubated for 24–72 h at 37 °C. The absorbance was measured at 450 nm (with a reference wavelength at 620 nm) by using a spectrophotometer (FLUOstar, BMG Labtech) 1–2 h after the addition of CCK-8 (10 μL).

Cellular uptake of the peptide-grafted cNDs: Intracellular localisation of the peptide-grafted cNDs was analysed by using a LEICA SPC2 (Mannheim, Germany) confocal laser scanning microscope with a 100× objective (NA 1.4). CHO-K1 cells were plated on glass coverslips (20000 cells, 1 cm^2) and cultured for 24 h. The cells were washed once with serum-free medium. NDs (0–50 μL of 0.2 g L^{-1} stock solutions) were incubated with cells in fresh serum-free DMEM medium (1 mL) for 60–120 min at 37 °C. Cells were washed with PBS (5×1 mL) before being fixed in 3% paraformaldehyde (20 °C, 10 min) and permeabilisation with Triton X-100 (0.1%) in PBS (20 °C, 5 min). Fixed cells were then incubated with phalloidin–TRITC (1:1000 in PBS; Invitrogen) to label cytosolic actin (20 °C, 45 min), TO-PRO-3 iodide (1:5000 in water; Invitrogen) to label nuclei (20 °C, 5 min) and mounted in Vectashield fluorescence mounting medium (Biovalley).

Confocal microscopy: Cells were visualised with a LEICA SP2 confocal laser scanning microscope with a 63× (NA 1.32) and a 100× (NA 1.4) objective. Reflection images were obtained simultaneously with the fluorescent images of peptide–NDs by using the same scanning laser beam (488 nm).

Acknowledgements

This work was supported by the European Commission: project Nano4Drugs, contract LSFC-CT-2005-019102, including a postdoctoral fellowship to S.V. C.M. thanks the CNRS for a postdoctoral fellowship. We thank Alain Adenier for IR spectroscopy.

Keywords: cellular uptake · cytotoxicity · nanostructures · peptides · surface coating

[1] M. E. Akerman, W. C. W. Chan, P. Laakkonen, S. N. Bhatia, E. Ruoslahti, *Proc. Natl. Acad. Sci. USA* **2002**, *99*, 12617- 12621.
[2] P. Alivisatos, *Nat. Biotechnol.* **2004**, *22*, 47–52.
[3] K. Kneipp, H. Kneipp, J. Kneipp, *Acc. Chem. Res.* **2006**, *39*, 443–450.
[4] R. Lévy, *ChemBioChem* **2006**, *7*, 1141–1145.
[5] J. A. Khan, B. Pillai, T. K. Das, Y. Singh, S. Maiti, *ChemBioChem* **2007**, *8*, 1237–1240.
[6] E. Nakamura, H. Isobe, *Acc. Chem. Res.* **2003**, *36*, 807–815.
[7] M. Prato, K. Kostarelos, A. Bianco, *Acc. Chem. Res.* **2008**, *41*, 60–68.
[8] A. Krueger, *Chem. Eur. J.* **2008**, *14*, 1382–1390.
[9] K. B. Holt, *Philos. Transact. A. Math. Phys. Eng. Sci* **2007**, *365*, 2845–2861.
[10] N. Kaji, M. Tokeshi, *Y. Baba, Chem. Rec.* **2007**, *7*, 295–304.
[11] S. J. Yu, M. W. Kang, H. C. Chang, K. M. Chen, Y. C. Yu, *J. Am. Chem. Soc.* **2005**, *127*, 17604–17605.
[12] K. K. Liu, C. L. Cheng, C. C. Chang, J. I. Chao, *Nanotechnology* **2007**, *18*, 325102.
[13] C. C. Fu, H. Y. Lee, K. Chen, T. S. Lim, H. Y. Wu, P. K. Lin, P. K. Wei, P. H. Tsao, H. C. Chang, W. Fann, *Proc. Natl. Acad. Sci. USA* **2007**, *104*, 727–732.
[14] A. M. Schrand, H. Huang, C. Carlson, J. J. Schlager, E. Osawa, S. M. Hussain, L. Dai, *J. Phys. Chem. B* **2007**, *111*, 2–7.
[15] Y. Sonnefraud, A. Cuche, O. Faklaris, J. P. Boudou, T. Sauvage, J. F. Roch, F. Treussart, S. Huant, *Cond. Mater.* **2007**, 1–8.
[16] L. C. Huang, H. C. Chang, *Langmuir* **2004**, *20*, 5879–5884.
[17] E. Perevedentseva, C. Y. Cheng, P. H. Chung, J. S. Tu, Y. H. Hsieh, C. L. Cheng, *Nanotechnology* **2007**, *18*, 315102 .
[18] H. Huang, E. Pierstorff, E. Osawa, D. Ho, *Nano. Lett.* **2007**, *7*, 3305–3314.
[19] P. H. Chung, E. Perevedentseva, J. S. Tu, C. C. Chang, C. L. Cheng, *Diamond Relat. Mater.* **2006**, *15*, 622–625.
[20] A. Krüger, Y. Liang, G. Jarre, J. Stegk, *J. Mater. Chem.* **2006**, *16*, 2322–2328.
[21] K. Ushizawa, Y. Sato, T. Mitsumori, T. Machinami, T. Ueda, T. Ando, *Chem. Phys. Lett.* **2002**, *351*, 105–108.
[22] C. Y. Cheng, E. Perevedentseva, J. S. Tu, P. H. Chung, C. L. Cheng, K. K. Liu, J. I. Chao, P. H. Chen, C. C. Chang, *Appl. Phys. Lett.* **2007**, *90*, 163903.
[23] S. Vial, I. Pastoriza-Santos, J. Perez-Juste, L. M. Liz-Marzan, *Langmuir* **2007**, *23*, 4606–4611.
[24] E. Kaiser, R. L. Colescott, C. D. Bossinger, P. I. Cook, *Anal. Biochem.* **1970**, *34*, 595–598.
[25] J. S. Tu, E. Perevedentseva, P. H. Chung, C. L. Cheng, *J. Chem. Phys.* **2006**, *125*, 174713.
[26] Y. Luo, P. Yang, J. Lin, *Micropor. Mesopor. Mater.* **2008**, *111*, 194–199.
[27] A. L. Morales-Cruz, E. R. Fachini, F. A. Miranda, C. R. Cabrera, *Appl. Surf. Sci.* **2007**, *253*, 8846–8857.
[28] S. J. Xiao, M. Wieland, S. Brunner, *J. Colloid Interface Sci.* **2005**, *290*, 172–183.
[29] S. F. Parker, *Spectrochim. Acta Part A* **2006**, *63*, 544–549.
[30] D. Delaroche, B. Aussedat, S. Aubry, G. Chassaing, F. Burlina, G. Clodic, G. Bolbach, S. Lavielle, S. Sagan, *Anal. Chem.* **2007**, *79*, 1932–1938.

Received: April 11, 2008
Published online on August 1, 2008

